INVESTIGATION OF MICROWAVE ALLOYING USING ELECTRON MICROSCOPY: SEGREGATION BETWEEN MANGANESE AND BISMUTH BY PERITECTIC REACTION

Chitnarong Sirisathitkul[1,2*], Thanida Charoensuk[1,3], Upsorn Boonyang[1,4], Dhammanoon Srinoum[5] and Mudtorlep Nisoa[2,5]

[1] Center of Excellence in Functional Materials and Nanotechnology, Walailak University, Nakhon Si Thammarat, 80160, Thailand
[2]Division of Physics, School of Science, Walailak University, Nakhon Si Thammarat, 80160, Thailand
[3]Thailand Center of Excellence in Physics, Ministry of Higher Education, Science, Research and Innovation, 328 Si Ayutthaya Road, Bangkok, 10400, Thailand
[4]Division of Chemistry, School of Science, Walailak University, Nakhon Si Thammarat, 80160, Thailand
[5]Center of Excellence in Plasma Science and Electromagnetic Waves (PEwave), Walailak University, Nakhon Si Thammarat, Thailand

*chitnarong.siri@gmail.com

Abstract. A microwave furnace combining the power of 2,000-2,500 W from 4 commercial magnetrons is demonstrated as an apparatus for melting alloys. Under an argon atmosphere, the microwave heating was transferred to pieces of broken bismuth (Bi) ingots and manganese (Mn) flakes via a silicon carbide plate for 1 h. Field-emission scanning electron microscopy (FESEM) and energy-dispersive X-ray spectroscopy (EDS) revealed inhomogeneous composition and morphology, similar to MnBi alloyed in arc-melting and induction furnaces. Due to the peritectic reaction, the product contained mixed phases of Mn, Bi, Bi_2O_3, and MnBi with particle size ranging from 100 nm to over 1 μm. Bulky cubic-like particles were unreacted Mn clusters, whereas fine particles were Bi and Bi_2O_3. Homogeneous regions among Mn-rich and Bi-rich particles were characterized as the MnBi phase. Areas with a balanced composition between Mn and Bi were increasingly observed after annealing at 280°C under the pressure of 60 psi for 12 h.

Keywords: microwave furnace, electron microscopy, peritectic reaction, MnBi, alloys

Article Info

Received 11th May 2021
Accepted 7th September 2021
Published 20th December 2021

ISSN: 1823-7010, eISSN: 2600-7444

Introduction

The applications of alloys are rapidly extended from traditional uses to advanced functions. Numerous combinations and compositions of metals are increasingly investigated for their mechanical and physical properties. Various alloying techniques using arc-melting, melt-spinning, and electromagnetic induction furnaces have been improved and modified to meet new demands regarding each functional alloy [1-3]. Microwave heating is ubiquitous in household, drying of agricultural products as well as chemical processes. Compared to other forms of heating, the microwave furnace is economical in terms of energy and time, resulting in extensive implementation with dielectric materials [3,4]. However, its use in alloy processing is somewhat limited since the microwave cannot directly heat bulk metals. Only microwave sintering of metallic powders is widely used because microwave does not reflect from powders [5,6].

In this work, a microwave furnace was developed as an alternative for alloying functional materials and tested in alloying manganese-bismuth (MnBi). This ferromagnetic alloy has been investigated for its positive temperature coefficients of coercivity [7] and magnetooptical properties [8]. The challenge in developing this rare-earth-free magnet is to synthesize the low-temperature phase (LTP) MnBi from precursors of highly different melting temperatures, i.e., 1246 °C for Mn and 271.4 °C Bi. Moreover, Mn tends to segregate from Bi by the peritectic reaction during the solidification resulting in mixed phases of MnBi, Mn-rich, and Bi-rich clusters in common melt products [7,9]. Field-emission scanning electron microscopy (FESEM), equipped with energy-dispersive X-ray spectroscopy (EDS), is principally used to investigate both morphology and elemental composition of the product alloyed in this microwave furnace. The variations in elemental compositions can be used to explain the partial formation of the LTP MnBi observed by X-ray diffractometry (XRD) and differential thermal analysis (DTA). The phase segregation is also observed in FESEM images.

Materials and Methods

Four commercial magnetrons (LCEL001B) were combined to raise microwave power to 2,000-2,500 W for the alloying in a stainless-steel cubic cavity (28×28×28 cm^3). The microwave irradiation through 2.17-3.30 GHz waveguides assembled on 4 sides of the cavity was converted into heat by a silicon carbide (SiC) plate. Metals can then be melted in an alumina crucible placed on the SiC heating plate, as depicted in Figure 1. To reduce the oxidation on the surface of alloys, the air was evacuated and the microwave cavity was then by argon gas before the alloying.

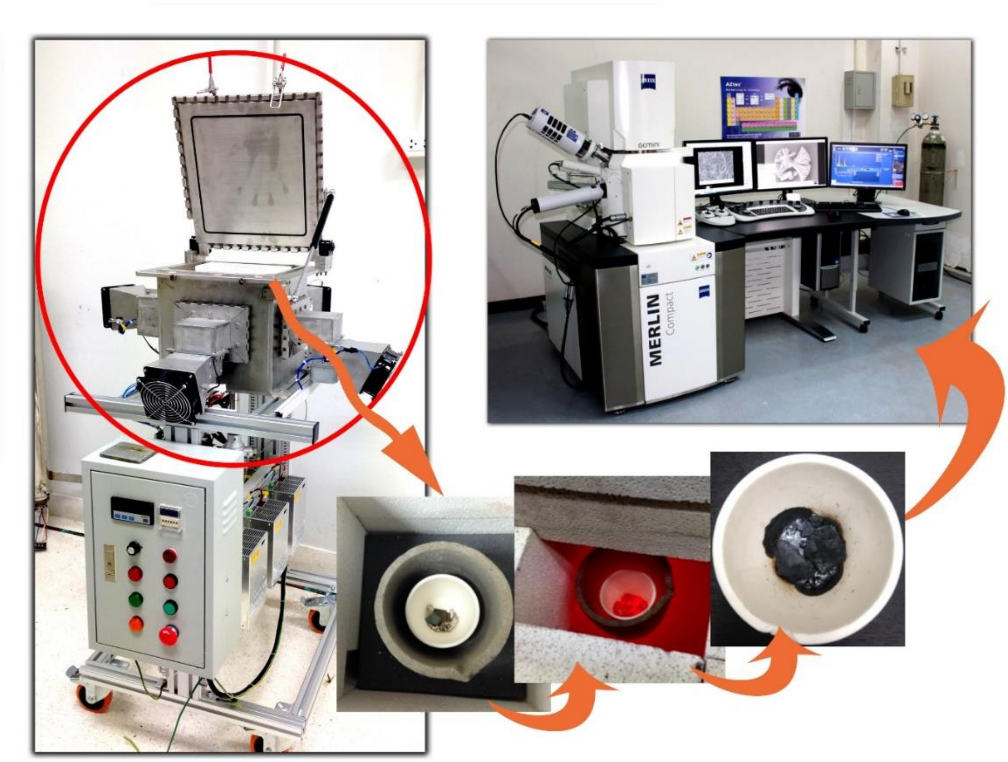

Figure 1. Alloying MnBi in microwave furnace and characterization by FESEM/EDS

The lab-made microwave furnace was tested by alloying Mn flakes (99.9%) and broken Bi ingot (99.99%) in the atomic ratio of 2:1. The melting was carried out at the average temperature of 1,300°C for 1 h. Then, magnetrons were switched off, allowing the alloyed product to cool down to room temperature before it was ground into powders. Thermal properties were measured by DTA (PerkinElmer DTA7) at the rate of 5°C/min. The other sample was prepared by annealing the as-melt sample at 280°C under the pressure of 60 psi for 12 h in a lab-made apparatus described in [10]. The morphology of ground products was visualized by the FESEM (Zeiss Merlin Compact). The elemental compositions on selected areas were probed by EDS (Oxford Aztec) attached to the FESEM, as shown in Figure 1. For the phase characterization, the single-crystal X-ray crystallography (Rigaku Oxford Diffraction-XtaLAB SuperNova) was operated in the micro powder mode using a Cu microfocus X-ray source and a HyPix 3000 detector.

Results and Discussion

A DTA curve in Figure 2 shows the absorption and release of heat, related to changes in structure and phase of the alloyed product. The broad endothermic peak under 100°C signifies water removal. The sharp endothermic peak at 274°C corresponds to the melting of Bi. A broad exothermic peak present below 400°C, consistent with the literature [11], is attributed to the formation of LTP MnBi. The LTP to high-temperature phase (HTP) and other endothermic transitions are observed as the temperature increases. Besides endothermic transitions, the crystallization results in a broad exothermic peak slightly below 1000°C. These thermal properties can confirm the characterizations by XRD and EDS.

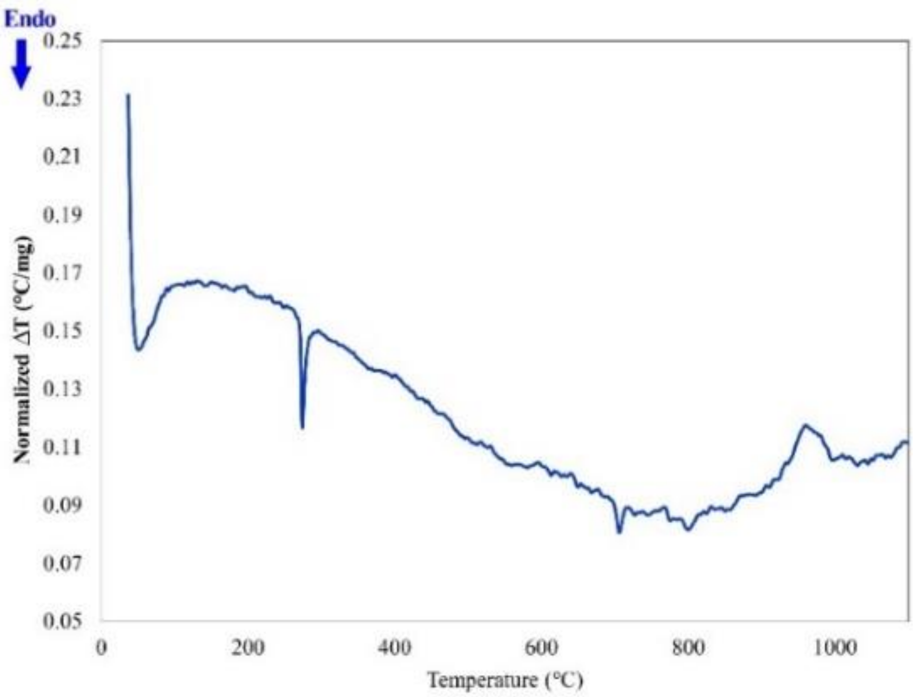

Figure 2. DTA curve of MnBi alloyed in the microwave furnace for 1 h.

EDS spectra from three regions compared in Figure 3 indicate that the alloyed product is highly inhomogeneous. The first exemplified region has the elemental Mn:Bi ratio of 28.82. By contrast, the light region has a much higher Bi composition than that of Mn, confirming the segregation between Mn and Bi. Finally, there are also somewhat homogeneous regions, but the Mn composition is still higher than Bi. By arc-melting Mn and Bi, the ratios of Mn:Bi were similarly varied [9]. The products previously obtained from arc-melting [12] and vacuum sintering [13] were also classified into three regions. Significant detections of oxygen and carbon can be attributed to the chamber environment [14]. Moreover, Mn is highly susceptible to oxidation.

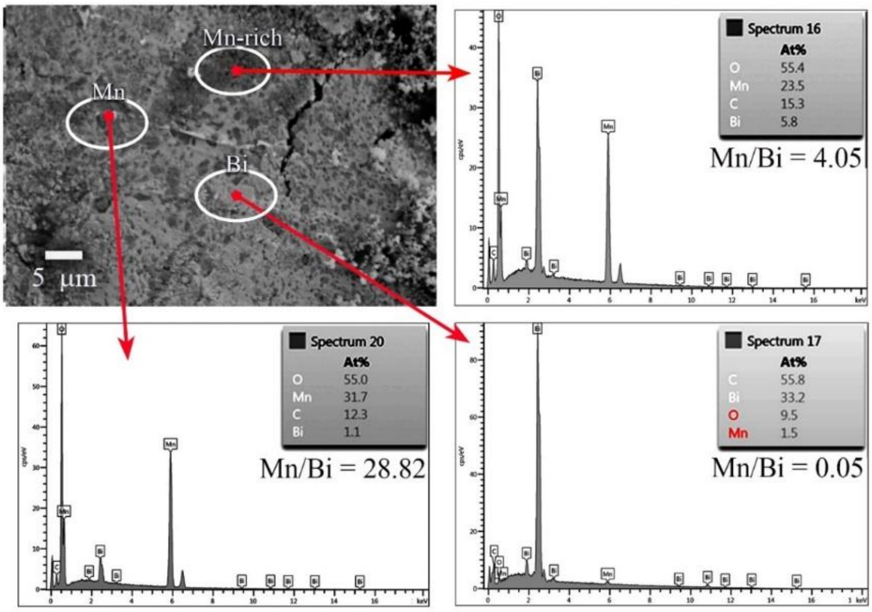

Figure 3. EDS spectra of the MnBi after melting in the microwave furnace for 1 h.

The XRD pattern of the product alloyed for 1 h displayed in Figure 4a exhibits the mixed phases of Mn, Bi, Bi_2O_3, C, and most importantly, MnBi. The strongest peak is indexed to Bi at 27.2°(012). Other peaks are also matched with the Bi standard (ICSD Reference: 01-085-1329). The peaks assigned to Mn are clearly displayed. In the previous reports, MnO peaks were not clearly observed by XRD [15] but detected by synchrotron X-ray absorption [16]. For the LTP MnBi phase, the peaks reveal at 28.1°(101), 23.9°(100), 29.2°(002), 38.0°(102), 42.1°(110), 51.2°(103), 51.4°(201), 52.1°(112), 58.1°(202), and 68.6°(211) (NIST Reference: 03-065-8164).

The phase distribution can be concluded from EDS and XRD results and matched with the morphology in the FESEM image. In Figure 4b, clusters of nanoparticles with irregular shapes and lighter appearance are Bi and Bi_2O_3. Darker granules of 0.5 -1 μm in size are Mn-rich. Their larger size and planar facets distinguish them from Bi-rich clusters. The MnBi phase is not clearly observed and has no distinct morphology. This inhomogeneity is attributed to the difference in melting temperature, and the peritectic reaction as the Mn tends to form solid clusters in the melted Bi matrix. Such phase segregations were similarly reported in the products from arc-melting [9,14,17], melt-spinning [18] and induction furnaces [19]. It was demonstrated that MnBi alloys could be homogenized by repeating the melting a few times [9,11,12].

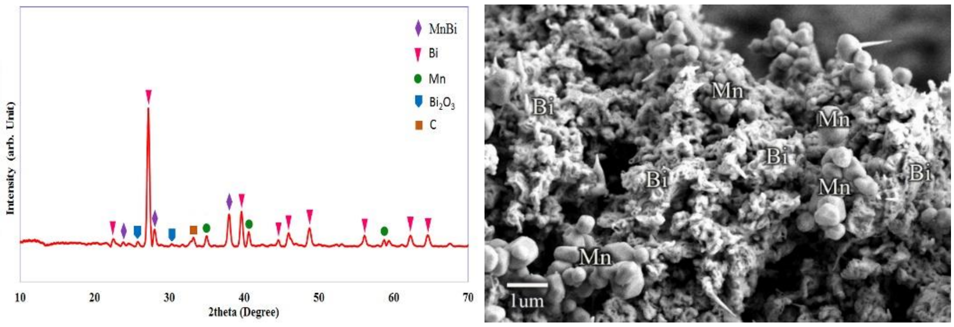

(a) **(b)**

Figure 4. (a) XRD spectrum and (b) FESEM image of the MnBi after melting in the microwave furnace for 1 h.

After the pressing-annealing for 12 h, the spatial distribution in the elemental composition of the product is exemplified by three EDS spectra in Figure 5. Whereas either large Mn or Bi composition over the other is still obtained, the Mn:Bi ratio is closer to 1 in some regions. The diffraction peaks in Figure 6a are present at the same positions, but characteristic MnBi peaks become stronger after the annealing. The crystallite size, calculated with the Scherrer equation, is around 22 nm for both before and after the annealing. The balanced Mn and Bi regions were obviously enhanced after the annealing, represented by the uniform surface on the FESEM image in Figure 6b. Bi-rich clusters of nanoparticle and Mn-rich granules still exist, but their segregation is reduced. The annealing effect on MnBi morphology is comparable to arc-melted products after the annealing at 300 °C [9]. During the annealing below the LTP-HTP transition point, reactions between Bi and Mn clusters enhance the LTP MnBi formation [7,14,18,20]. However, the annealing at a higher temperature of 500 °C for 48 h was detrimental to the LTP MnBi [8].

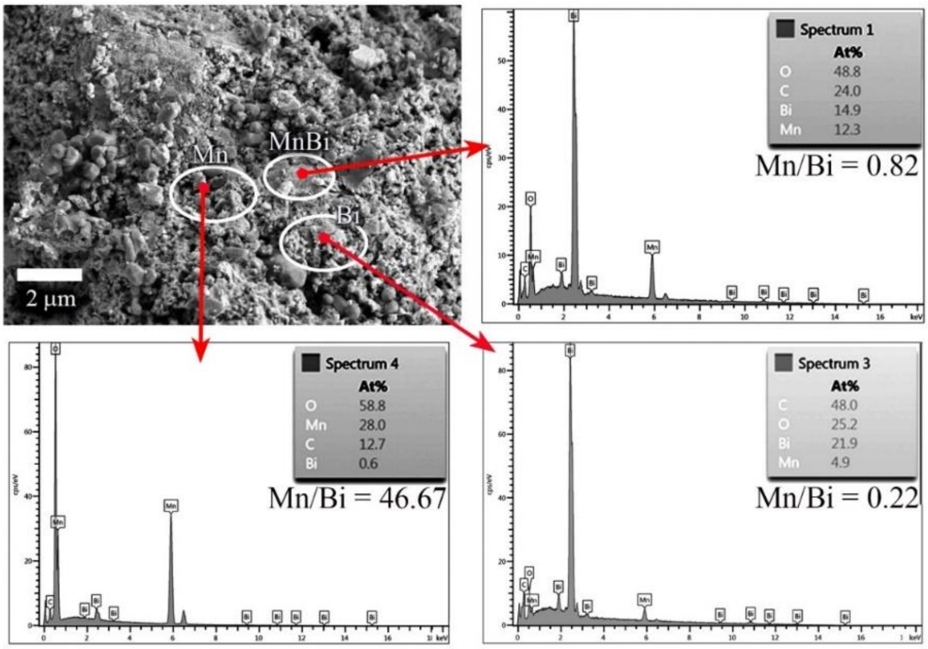

Figure 5. EDS spectra of the MnBi obtained after annealing at 280°C, 60 psi for 12 h.

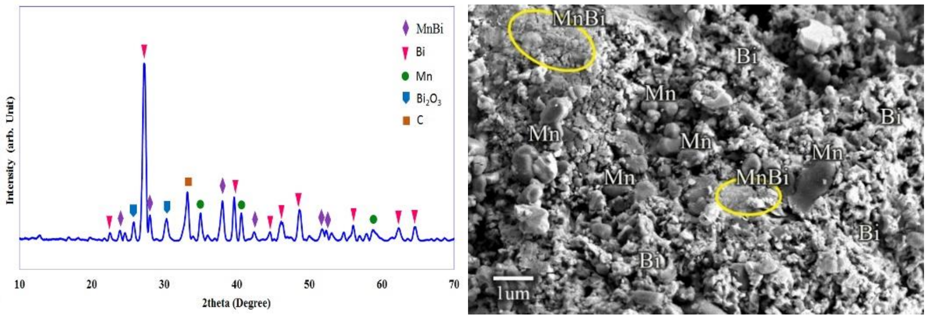

(a) **(b)**

Figure 6. (a) XRD spectrum and (b) FESEM image of the MnBi obtained after annealing at 280°C, 60 psi for 12 h.

Conclusion

Four commercial magnetrons were combined to raise the temperature in the microwave furnace to over the melting point of Mn. According to characterizations by FESEM and EDS, the melting of Mn with Bi, whose melting temperature was much lower, resulted in a highly inhomogeneous alloyed product. The annealing at 280 °C under the pressure of 60 psi for 12 h homogenized the alloys. The balanced Mn and Bi regions shown by EDS and uniform morphology shown by FESEM were enlarged. In addition to the investigation of phase segregation by electron microscopy, this microwave heating was successful in producing alloyed products from metals with highly different melting points and can be extended to manufacture several other alloys.

Acknowledgments

This work is financially supported by the Thailand Center of Excellence in Physics (Grant No. ThEP-63-PIP-WU3). Technical assistance by P. Sukonrat, P. Thongjumpa and P. Saetang are acknowledged.

Author Contributions

All authors contributed toward data analysis, drafting, and critically revising the paper and agree to be accountable for all aspects of the work.

Disclosure of Conflict of Interest

The authors have no disclosures to declare.

Compliance with Ethical Standards Conclusions

The work is compliant with ethical standards.

References

[1] Gertsyk, S. I. & Smirnova, V. A. (2019). Technology of melting an invar in an induction furnace. *Russian Metall.* 2019(6) 647-650.

[2] Sivtsov, A. V., Sheshukov, O. Y., Tsymbalist, M. M., Nekrasov, I. V., Makhnutin, A. V., Egiazar'yan, D. K. & Orlov, P. P. (2018). Steel semi-product melting intensification in electric arc furnaces using coordinated control of electric and gas conditions: I. heat exchange and structure of the electric arc furnace laboratory. *Russian Metall.* 2018(12) 1108-1113.

[3] Biesuz, M., Saunders, T., Ke, D., Reece, M. J., Hu, C. & Grasso, S. (2021). A review of electromagnetic processing of materials (EPM): Heating, sintering, joining and forming. *J. Mater. Sci. Technol.* 69 239-272.

[4] Na, T. W., Pabli, F. A. M., Sharifuddin, S. M., Nor, M. S. M., Wan Ali, W. F. F. & Sulaiman, M. A. (2020). Effect of calcination time on the microstructure and dielectric properties of $CaCu_3Ti_4O_{12}$ using enhanced microwave processing. *Malay. J. Microsc.* 16(1) 83-93.

[5] Annamalai, R., Upadhyaya, A. & Agrawal, D. (2013). An investigation on microwave sintering of Fe, Fe–Cu and Fe–Cu–C alloys. *Bull. Mater. Sci.* 36(3) 447-456.

[6] Rajesh, R., Shankar, B., Harikrishnan, J., Ritwik, A., Hari Krishna, A., Usman, Q. & Hari Sankar, R. (2020). Study on conventional and microwave-assisted sintering of Cu-FA composites. *Mater. Today Proc*. 39(4) 1677-1681.

[7] Sarkar, A. & Mallick, A. B. (2020). Synthesizing the hard magnetic low-temperature phase of MnBi Alloy: Challenges and prospects. *JOM* 72(8) 2812-2825.

[8] Christopher, N. R., Singh, N., Singh, S. K., Gahtori, B., Mishra, S. K., Dar, A. & Awana, V. P. S. (2013). Appreciable magnetic moment and energy density in single-step normal route synthesized MnBi. *J. Supercond. Novel Magn.* 26 3161-3165.

[9] Nguyen, V. V. & Nguyen, T. X. (2018). Effect of microstructures on the performance of rare-earth-free MnBi magnetic materials and magnets. *Phys. B: Condens. Matter* 532 103-107.

[10] Charoensuk, T., Tamman, A., Jantaratana, P., Abbasi, S. & Sirisathitkul, C. (2019). One step pressing-annealing to produce LTP MnBi magnets. *J. Met. Mater. Miner.* 29(2) 105-109.

[11] Anand, K., Christopher, N. & Singh, N. (2019). Evaluation of structural and magnetic property of Cr-doped MnBi permanent magnet material. *Appl. Phys. A* 125 870.

[12] Nguyen, V. V. & Nguyen, T. X. (2017). An approach for preparing high-performance MnBi alloys and magnets. *J. Electron. Mater.* 46(6) 3333-3340.

[13] Ngamsomrit, S., Saisopa, T., Borsup, J., Tun, M. S., Myint, H. T., Nakajima, H., Songsiriritthigul, C., Pinitsoontorn, S. & Songsiriritthigul, P. (2021). Preparation of low-temperature phase MnBi by sintering in vacuum. *J. Phys.: Conf. Ser.* 1719 012057.

[14] Li, B., Ma, Y., Shao, B., Li, C., Chen, D., Sun, J. C., Zheng, Q. & Yin, X. (2018). Preparation and magnetic properties of anisotropic MnBi powders. *Phys. B: Condens. Matter* 530 322-326.

[15] Xie, W., Polikarpov, E., Choi, J., Bowden, M. E., Sun, K. & Cui, J. (2016). Effect of ball milling and heat treatment process on MnBi powders magnetic properties. *J. Alloys Compd.* 680 1-5.

[16] Sirisathitkul C. & Charoensuk T. (2019). Effects of composition and heat treatment on manganese-bismuth magnets. *Micro & Nano Lett.* 14(6) 661-664.

[17] Betancourt, I., Zamora, J., Jiménez, A., del Real, R. P. & Vázquez M. (2018) Rare earth-free hard magnetic microwires. *Script. Mater.* 153 40-43.

[18] Moon, K. W., Jeon, K.-W., Kang, M., Kang, M.-K., Byun, Y., Kim, J. B., Kim, H. & Kim, J. (2014). Synthesis and magnetic properties of MnBi(LTP) magnets with high-energy product. *IEEE Trans. Magn.* 50(11) 2103804.

[19] Xiang, Z., Wang, T., Ma, S., Qian, L., Luo, Z., Song, Y., Yang, H. & Lu, W. (2018). Microstructural evolution and phase transformation kinetics of MnBi alloys. *J. Alloys Compd.* 741 951-956.

[20] Cui, J., Choi, J. P., Polikarpov, E., Bowden, M. E., Xie, W., Li, G., Nie, Z., Zarkevich, N., Kramer, M. J. & Johnson, D. (2014). Effect of composition and heat treatment on MnBi magnetic materials. *Acta Mater.* 79 374-381.